Conformational signaling required for synaptic plasticity by the NMDA receptor complex

Jonathan Aow[1], Kim Dore[1], and Roberto Malinow[2]

Center for Neural Circuits and Behavior, Department of Neuroscience and Section for Neurobiology, Division of Biology, University of California, San Diego, CA 92093

Contributed by Roberto Malinow, October 9, 2015 (sent for review September 8, 2015)

The NMDA receptor (NMDAR) is known to transmit important information by conducting calcium ions. However, some recent studies suggest that activation of NMDARs can trigger synaptic plasticity in the absence of ion flow. Does ligand binding transmit information to signaling molecules that mediate synaptic plasticity? Using Förster resonance energy transfer (FRET) imaging of fluorescently tagged proteins expressed in neurons, conformational signaling is identified within the NMDAR complex that is essential for downstream actions. Ligand binding transiently reduces FRET between the NMDAR cytoplasmic domain (cd) and the associated protein phosphatase 1 (PP1), requiring NMDARcd movement, and persistently reduces FRET between the NMDARcd and calcium/calmodulin-dependent protein kinase II (CaMKII), a process requiring PP1 activity. These studies directly monitor agonist-driven conformational signaling at the NMDAR complex required for synaptic plasticity.

long-term depression | LTD | NMDAR-PP1 FRET | NMDAR-CaMKII interaction | ion-flow independent

Agonist binding to the NMDAR is required for two major forms of synaptic plasticity: long-term potentiation (LTP) and long-term depression (LTD) (1). Surprisingly, activation of NMDARs can produce plasticity in opposite directions, with LTP enhancing transmission and LTD reducing transmission. A model was developed (2, 3) to explain how activation of NMDAR could produce these opposing phenomena: strong stimuli during LTP induction drive a large flux of Ca^{2+} through NMDARs, leading to a large increase in intracellular calcium ion concentration ($[Ca^{2+}]_i$) that activates one series of biochemical steps leading to synaptic potentiation; a weaker stimulus during LTD induction drives a more reduced flux of Ca^{2+} through NMDARs, producing a modest increase in $[Ca^{2+}]_i$ that activates a different series of biochemical steps, leading to synaptic depression. However, this model is not consistent with recent studies suggesting that no change in $[Ca^{2+}]_i$ is required for LTD, and instead invokes metabotropic signaling by the NMDAR (4). Studies supporting an ion-flow-independent role for NMDARs in LTD (4–7) and other processes (7–13) stand in contrast to studies proposing that flow of Ca^{2+} through NMDAR is required for LTD (14) (see ref. 15 for additional references). An important test of an ion-flow-independent model would be to measure directly signaling actions by NMDARs in the absence of ion flow.

Results

Transient NMDAR Agonist Binding Without Ion Flux Depresses Spontaneous Excitatory Postsynaptic Currents. In the accompanying study (16), Förster resonance energy transfer (FRET)-fluorescence lifetime imaging microscopy (FLIM) imaging was used to show that agonist binding to the NMDAR produces conformational movement of the NMDARcd. This effect displayed the same pharmacological profile as the electrically induced LTD recently published (4) and independently confirmed (7), suggesting that the conformational changes measured in the NMDARcd are associated with LTD induction. To test whether the stimulation protocol that drives conformational changes in the NMDARcd produces changes in synaptic function, spontaneous synaptic activity was recorded in primary hippocampal neurons, and NMDA was transiently applied in the presence of 7CK, a noncompetitive NMDAR antagonist that effectively blocks NMDAR currents (Fig. S1), under the same conditions as used for FLIM. Analysis of spontaneous synaptic events (in a manner blind to treatment conditions) showed a significant reduction in the frequency and amplitude of spontaneous synaptic events 15 min after NMDA washout (Fig. 1). This synaptic depression was significantly reduced when NMDA was applied with 2-amino-5-phosphonopentanoic acid (APV) in the bath (Fig. 1 *A*–*C*), or if no NMDA was applied to neurons bathed in 7CK or APV (Fig. 1 *A*–*C*). Therefore, in dissociated cultured neurons, NMDA application in the presence of 7CK results in depressed synaptic function, consistent with LTD. In control experiments, recordings of neuronal holding currents displayed an increase on application of NMDA that was blocked by 7CK, indicating an effective block of ion flux through NMDARs (Fig. S1; see also figure S4 in ref. 16). These results reinforce the conclusion that NMDARs possess agonist-driven and ion-flux-independent activity sufficient to depress synaptic function.

Next, we examined whether ligand-driven NMDAcd movement is required for the observed effects on synaptic function. To address this issue, we infused neurons with a patch pipette containing an antibody targeting the GluN1 cytoplasmic domain (cd) (or an anti-rabbit antibody as a control; Fig. 1 *D*–F), which would be expected to bind and immobilize two nearby GluN1cds; in the accompanying manuscript, data are presented indicating such infusion blocks an agonist-driven change in GluN1-GFP lifetime in neurons expressing GluN1-GFP/GluN1-mCherry/GluN2B (16). Infusion of GluN1cd antibody [but not control antibody, which does not prevent NMDARcd movement (16)] blocked NMDA-induced synaptic depression in the presence of 7CK (Fig. 1 *D*–*F*). The frequency and

Significance

Neurotransmitter binding to NMDA receptors (NMDARs) produces an ion-flow-independent conformational change in its intracellular domain, as well as synaptic depression. An antibody that blocks this movement also blocks ion-flow-independent synaptic depression. The interactions of the NMDAR with signaling proteins that mediate synaptic depression, protein phosphatase 1 (PP1), and calcium-calmodulin-dependent protein kinase II (CaMKII) are monitored using fluorescence lifetime imaging microscopy (FLIM) to measure Förster resonance energy transfer (FRET). Ligand binding to the NMDAR produces changes in these interactions that require conformational movement, but not ion flow through the receptor. Our study directly measures metabotropic signaling actions by NMDARs and provides insights into the mechanisms of synaptic depression.

Author contributions: J.A., K.D., and R.M. designed research; J.A. and K.D. performed research; J.A. and K.D. analyzed data; and J.A., K.D., and R.M. wrote the paper.

The authors declare no conflict of interest.

[1]J.A. and K.D. contributed equally to this work.

[2]To whom correspondence should be addressed. Email: rmalinow@ucsd.edu.

This article contains supporting information online at www.pnas.org/lookup/suppl/doi:10.1073/pnas.1520029112/-/DCSupplemental.

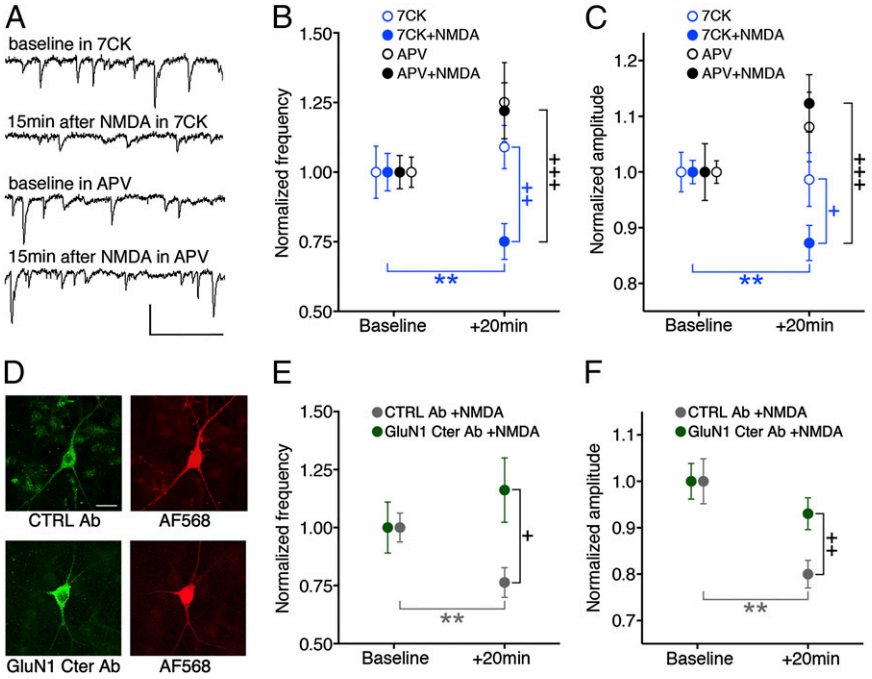

Fig. 1. Transient NMDA application produces reduced transmission in absence of ion flow through NMDARs blocked by an antibody to GluN1 C-terminal domain (GluN1 Cter Ab). (*A*) Representative traces of spontaneous EPSCs from primary hippocampal neurons at indicated times and conditions. (Scale bar, 50 pA, 100 ms.) (*B* and *C*) Plot of spontaneous EPSC frequency (*B*) or amplitude (*C*), normalized (to baseline period) at indicated times and conditions; N (neurons) for 7CK 16, +NMDA 23; APV 15, +NMDA 15. (*D*) Representative images of neurons infused with fluorescent control (CTRL) Ab (*Top*) or with GluN1 Cter Ab, immunostained with fluorescent secondary Ab (*Bottom*), along with red dye (*Right*). (Scale bar, 20 μm.) (*E* and *F*) Plot of spontaneous EPSC frequency (*E*) or amplitude (*F*) (normalized to baseline period) 20 min after NMDA application in 7CK for neurons infused with CTRL Ab ($n = 14$) or GluN1 Cter Ab ($n = 15$). $^{+}P < 0.05$, $^{++}P < 0.01$, $^{+++}P < 0.001$ compared between conditions (Mann–Whitney); $^{**}P < 0.01$ compared with baseline value (Wilcoxon).

amplitude of spontaneous events were similar with and without antibody infusion, suggesting this procedure had no effect on synaptic transmission (Fig. S2). These results support the view that movement of the NMDARcd is required for NMDA to produce ion-flux-independent synaptic depression. We cannot rule out the possibility that the binding of antibody to the NMDARcd has additional effects. However, as shown here, infusion of the antibody targeting GluN1cd did not affect baseline FRET efficiency between GluN1-GFP and an associated signaling molecule, supporting the view that the antibody did not block synaptic depression by displacing signaling molecules from the NMDARcd.

NMDA Drives FRET Changes Between Protein Phosphatase-1 and the NMDARcd. We hypothesized that agonist-driven conformational changes in the NMDARcd could activate nearby signaling molecules that mediate LTD. Protein phosphatase-1 (PP1) binds the NMDAR complex (17), and its activity is required for LTD (18). We thus expressed mCherry-tagged PP1 (PP1-mCherry), GluN1-GFP, and GluN2B in hippocampal neurons and examined FRET in spines before and during bath application of NMDA in the presence of 7CK. As in the accompanying study (16), GluN1-GFP lifetimes in individual spines were measured over time (spine lifetime in NMDA − spine lifetime before NMDA); these differences were then averaged to generate an average NMDA-driven change in spine GluN1-GFP lifetime. In baseline conditions, significant levels of FRET were detected between PP1-mCherry and GluN1-GFP in spines (3.2 ± 0.2% FRET efficiency; $n = 737$; $P < 0.0001$; table S1 in ref. 16), confirming close association of these molecules. During bath application of NMDA, a significant increase in GluN1-GFP lifetime was detected, which decayed to baseline levels within a few minutes of NMDA washout (Fig. 2). The increase in GluN1-GFP lifetime was blocked by APV, but not by okadaic acid, an inhibitor of PP1 activity (Fig. 2). These results are consistent with a transient change in location and/or orientation of PP1 within the NMDAR complex driven by NMDA-induced conformational changes in the NMDARcd, which could potentially expose the catalytic site on PP1 to a target substrate not available in baseline conditions.

We next tested whether conformational movement of the NMDARcd is required for the NMDA-induced reduced FRET efficiency observed between GluN1-GFP and PP1-mCherry. Neurons expressing these constructs were infused with the anti-GluN1cd antibody that blocked NMDA-induced change in intra-receptor FRET efficiency and synaptic depression (or the control anti-rabbit antibody). Although neurons infused with the control antibody displayed an NMDA-induced increased GluN1-GFP lifetime in 7CK, neurons infused with the antibody targeting GluN1cd did not (Fig. 2). Notably, infusion of the anti-GluN1cd antibody did not affect basal FRET between GluN1-GFP and PP1-mCherry (FRET efficiency was 3.4 ± 0.3% with GluN1cd Ab and 3.2 ± 0.2% with control antibody; $P = 0.4$, unpaired t test). These data suggest that movement of the NMDARcd is required for NMDA-driven reduced FRET efficiency between GluN1-GFP and PP1-mCherry.

NMDA Drives Dephosphorylation and Movement of Calcium/Calmodulin-Dependent Protein Kinase II Bound to NMDARcd. One potential target substrate of PP1 is the calcium/calmodulin-dependent protein kinase II (CaMKII) (19), which increases its binding to the NMDARcd after a rise in cytoplasmic Ca^{2+} (20), as produced during LTP stimuli (21). The binding of CaMKII to the NMDARcd confers autonomous CaMKII activity (20) and promotes LTP expression (22). To examine the effect of NMDA application on NMDAR-bound CaMKII, GluN1-GFP, mCherry-tagged CaMKII (CaMKII-mCherry), and GluN2B were expressed in neurons. In baseline conditions, a significant amount of FRET was observed

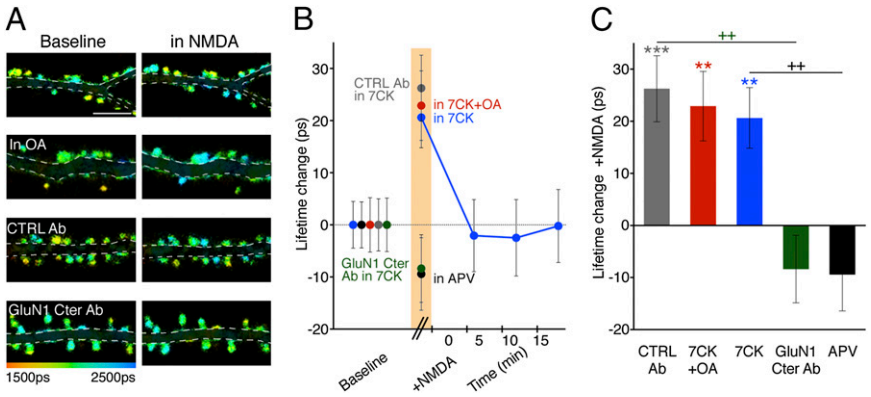

Fig. 2. NMDA drives FRET changes between PP1 and the NMDARcd. (*A*) Representative FLIM images of neurons expressing GluN1-GFP/PP1-mCherry at indicated times and conditions. OA (1 μM), okadaic acid. (*B*) Plot of GluN1-GFP lifetime change, relative to baseline, before, during (orange bar), and after NMDA application. N >15 neurons; > 400 spines per condition. (*C*) Bar graph of GluN1-GFP lifetime change, relative to baseline, during NMDA application for the indicated conditions. N > 15 neurons; > 400 spines per condition. $^{++}P < 0.01$ compared between conditions (Mann–Whitney); $^{**}P < 0.01$, $^{***}P < 0.001$ compared with baseline value (Wilcoxon).

between GluN1-GFP and CaMKII-mCherry (3.6 ± 0.2% FRET efficiency; $n = 622$; $P < 0.0001$; table S1 in ref. 16). NMDA was briefly bath applied, as earlier, in the presence of 7CK. Although during the application and immediately after washout of NMDA, little change in GluN1-GFP lifetime was observed, about 10 min after NMDA washout, a significant increase in GluN1-GFP lifetime was observed that persisted for the duration of the experiment (~20 min; Fig. 3 *A*–*C*). This change in GluN1-GFP lifetime was blocked by okadaic acid and APV (Fig. 3 *A*–*C*), indicating that PP1 activity and agonist binding to the NMDAR are required. Although okadaic acid blocks both PP2A and PP1, the paucity of PP2A at synapses has been used to conclude that okadaic acid blocks PP1 in synaptic processes (19, 23). The increased GluN1-GFP lifetime indicates a change in the location and/or orientation of CaMKII relative to the NMDARcd.

We tested whether dephosphorylation of phosphorylated threonine 286 on CaMKII (CaMKII-Thr286) is required for the agonist-driven change of NMDARcd-bound CaMKII. This site on CaMKII becomes phosphorylated (24) and is important for LTP (25) and

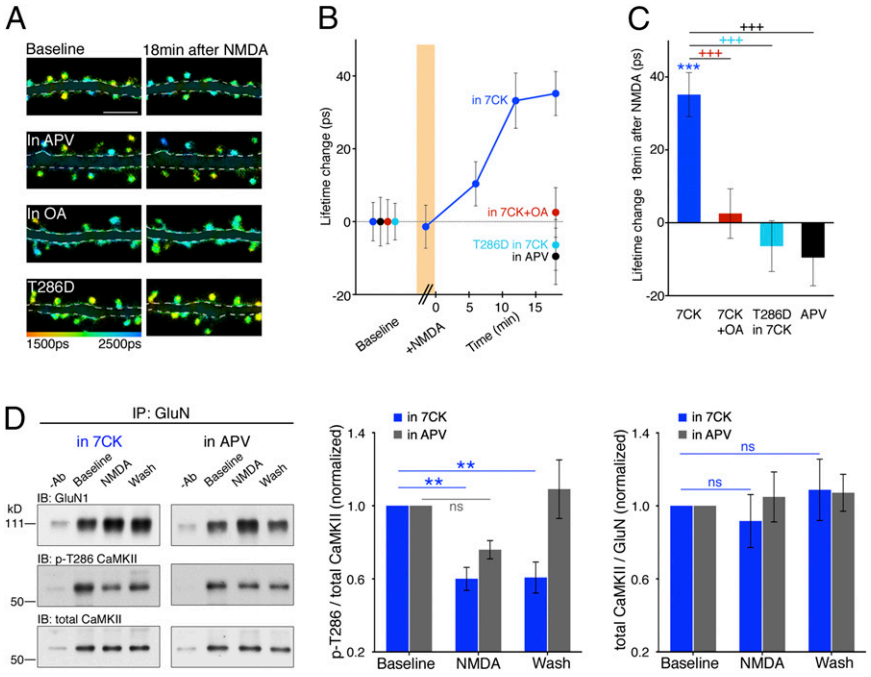

Fig. 3. NMDA drives dephosphorylation and movement of CaMKII bound to NMDARcd. (*A*) Representative FLIM images of neurons expressing GluN1-GFP/CaMKII-mCherry at indicated times and conditions. T286D indicates Thr286Asp mutant of CaMKII. (*B*) Plot of GluN1-GFP lifetime change, relative to baseline, before, during (orange bar), and after NMDA application. N > 16 neurons; > 400 spines per condition. (*C*) Bar graph of GluN1-GFP lifetime change, relative to baseline, during NMDA application for the indicated conditions. N > 16 neurons; > 400 spines per condition. (*D*, *left*) Representative immunoblots (IB) of GluN1, phospho-CaMKII-Thr286 (p-T286), and total CaMKII from cortical neuronal lysates coimmunoprecipitated with a GluN1 or GluN2B antibody under the indicated conditions. –Ab, no primary antibody during immunoprecipitation. (*Middle*) Average p-T286/total CaMKII for the indicated conditions; $n \geq 6$ experiments, including GluN1 or GluN2B for IP. (*Right*) Average total CaMKII levels relative to GluN1 or GluN2B. ns, not significant. $^{+++}P < 0.001$ compared between conditions (Mann–Whitney); $^{**}P < 0.01$, $^{***}P < 0.001$ compared with baseline value (Wilcoxon).

contributes to the autonomous activity and NMDAR-binding of CaMKII (reviewed in ref. 26). We examined mCherry-tagged CaMKII containing an aspartate at Thr286 (CaMKII-T286D-mCherry), which mimics a constitutively phosphorylated residue (27) that cannot be modified by phosphatase activity. Spines in neurons expressing GluN1-GFP, CaMKII-T286D-mCherry, and GluN2B displayed similar levels of FRET as spines coexpressing CaMKII-mCherry (Fig. 3 *A*–*C*). Bath application of NMDA in the presence of 7CK produced no increase in GluN1-GFP lifetime relative to baseline levels (Fig. 3 *A*–*C*), suggesting that dephosphorylation of phosphorylated CaMKII-Thr286 is required for the agonist-induced change of CaMKII relative to the NMDARcd during LTD (28).

To distinguish whether dephosphorylation of CaMKII-Thr286 after NMDA application leads to reorientation of CaMKII within the NMDARcd or removal of CaMKII from the NMDARcd, we performed coimmunoprecipitation experiments on native NMDARs. Dissociated cultured neurons were first incubated in 7CK, after which NMDA was applied (as in the imaging experiments) and then removed. The NMDAR complex was immunoprecipitated with an antibody to GluN1 or GluN2B and the immunoprecipitates analyzed by Western blot, initially probing with a phosphospecific antibody recognizing phospho-CaMKII-Thr286 before being stripped and reprobed with an antibody against CaMKII. Before NMDA application, a significant amount of CaMKII and phospho-CaMKII-Thr286 was associated with GluN1 or GluN2B. In the presence of 7CK (but not in the presence of APV), there was about 40% reduction in phospho-CaMKII-Thr286 during and after NMDA application, with no reduction in total CaMKII associated with the NMDAR complex (Fig. 3*D*). These results support the view that agonist binding to the NMDAR leads to the PP1-driven dephosphorylation and reorientation of CaMKII bound to the NMDARcd (Fig. 4).

Discussion

NMDARs can transmit information by transmembrane passage of calcium ions (29). In addition, a few reports suggest that ligand binding to NMDARs can produce synaptic (4–7) and cellular (7–13) effects in the absence of ion flux. An accompanying study showed that agonist binding to the NMDAR leads to a rapid ion-flow-independent conformational change in its cytoplasmic domain (16). Here we examined signaling downstream of such conformational change in the NMDAR cytoplasmic domain that is required for synaptic depression.

We find that bath NMDA application to dissociated cultured neurons, as has been used to model LTD (30, 31), produces a reduction in frequency and amplitude of spontaneous excitatory postsynaptic currents (EPSCs) in the presence of 7CK. This effect is blocked by APV, as well as intracellular infusion with an antibody targeting the intracellular domain of GluN1. These results support the view that ion-flux-independent activity by NMDAR can drive conformational signaling mediated by its cytoplasmic domain sufficient to produce synaptic depression.

We also find that ligand binding produces a transient change in the interaction between the NMDARcd and PP1, requiring movement of the NMDARcd, potentially allowing PP1 to act on phosphorylated CaMKII-Thr286. It is notable that phosphorylated CaMKII-Thr286 in postsynaptic densities (PSDs) can be dephosphorylated by soluble PP1, but is not accessible to PP1 that is embedded in PSDs, indicating structural constraints could affect the ability of PSD-PP1 to dephosphorylate PSD-CaMKII (32,33) that may be relieved by agonist binding to the NMDAR during LTD. NMDA binding also reduced the interaction between the NMDARcd and CaMKII that was delayed but persistent and blocked by PP1 inhibition. The delay may indicate that several Thr286 sites on the CaMKII complex, which normally exists as a 12-subunit holoenzyme (34, 35), require dephosphorylation for the holoenzyme to move with respect to the NMDARcd. Our immunoprecipitation experiments support the view that agonist binding to the NMDAR leads to Thr286 dephosphorylation of associated CaMKII without its unbinding to the NMDARcd, suggesting a reorientation of CaMKII within the complex to a new location, maintaining catalytic activity (20) with potentially different substrates, necessary for LTD (28, 36).

Materials and Methods

Procedures involving fluorescence lifetime imaging, FRET calculations, chemicals and reagents, primary culture preparation, transfection, image analysis (see also Fig. S3), and statistics are detailed in ref. 16.

Electrophysiology. Spontaneous excitatory postsynaptic currents (sEPSCs) were recorded from DIV 8–14 primary hippocampal neurons held at −60 mV in blocking HBSS solution. A standard cesium methanesulfonate internal solution (containing, in mM, 115 cesium methanesulfonate, 20 CsCl, 10 Hepes, 2.5 $MgCl_2$, 4 Na_2ATP, 0.4 Na_3GTP, 10 sodium phosphocreatine, 0.6 EGTA, and 0.1 spermine at pH 7.25) was used for all electrophysiology experiments. In experiments examining synaptic function, neurons were kept in regular HBSS solution for ∼15–30 min followed by wash-in of blocking HBSS solution containing either 50 μM 7CK or 100 μM APV. Antagonists were applied for at least 15 min before recordings were made. A 5-min baseline of spontaneous activity was recorded before NMDA application (25 μM NMDA for ∼5 min). Activity was subsequently recorded for ∼15 min after NMDA washout. APV-alone values in Fig. 1 include experiments in which APV was added after a baseline was obtained ($n = 10$) and continuous measurements in APV ($n = 6$); they did not differ and were thus pooled. 7CK-alone values are all from continuous measurements in 7CK. sEPSCs were analyzed

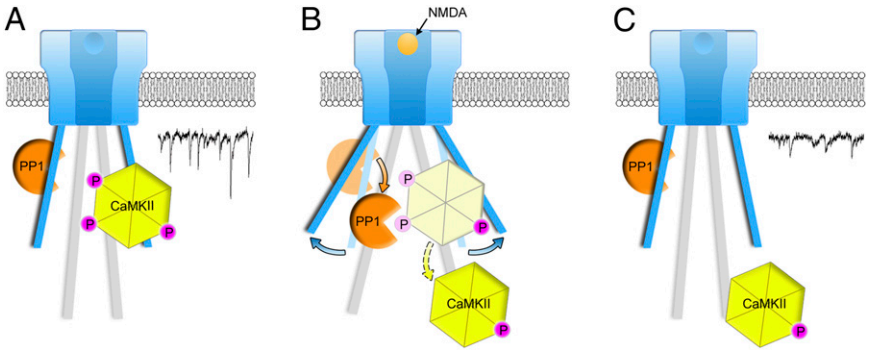

Fig. 4. Model consistent with imaging, electrophysiological, and biochemical data. (*A*) CaMKII phosphorylated (P) at Thr286 and PP1 bound to NMDAR-complex; PP1 lacks catalytic access to phospho-CaMKII-T286; in this conformation, NMDAR-complex signaling maintains basal transmission (trace). (*B*) NMDARcd moves permitting PP1 catalytic access to phospho-CaMKII-T286. (*C*) CaMKII lacking phosphate on Thr286 is relocated on the NMDARcd, which returns to baseline conformation; CaMKII, along with other signaling molecules activated by metabotropic NMDAR signaling, contributes to synaptic depression (trace). Trace examples taken from Fig. 1*A*.

manually using the MiniAnalysis program (Synaptosoft) blind to experimental conditions; event threshold was set at 6–8 pA. For each neuron, the frequency and amplitude of events during the 11–15-min period after NMDA washout were analyzed and normalized to the 5-min baseline period.

For holding current experiments (Fig. S1), cells were held at −60 mV for 1 min before the holding potential was gradually adjusted to +40 mV. The holding potential was monitored for 1 min before 25 μM NMDA was washed in. Holding currents were then monitored during a 7-min period. Analysis of currents was done using Igor (Wavemetrics).

Infusion of GluN1 C-Terminal Antibody into Neurons. A GluN1 C-terminal domain antibody (MAB1570) was introduced into neurons via a patch pipette. The cesium-based internal solution was supplemented with the GluN1 C-terminal antibody or the control antibody (GAR-AF488 for Fig. 1 and GAR-AF647 for Fig. 2) to a 20 μg/mL concentration, and the osmolality was adjusted (to ∼290 mOsm/kg) to compensate for the higher osmolality of the antibody solution. For the electrophysiology measurements shown in Fig. 2, the antibody was infused into neurons for a 7-min period before recording the 5-min baseline, so the antibody could diffuse into patched neurons for 12 min before NMDA application. For the experiments shown in Fig. 2, neurons were patched under the FLIM microscope for ∼10 min and were imaged after 30–60 min to allow for both increased antibody diffusion along the dendrites and the ability to image more than one neuron per experiment (maximum of three neurons; see figure S4*A* in ref. 16).

Immunohistochemistry. To facilitate localization of patched neurons and to verify antibody diffusion after imaging, a water-soluble red dye [Alexa Fluor 568 Hydrazide (Life Technologies), dissolved in water and used at a final concentration of 5 μM] was also included in the internal solution. When a control antibody was used, neurons were fixed in 4% (vol/vol) paraformaldehyde in PBS directly after electrophysiology for 10 min and then washed in PBS and mounted onto microscope slides using Prolong Gold antifade mounting media (Life Technologies). When the GluN1-C terminus antibody was used, neurons were first fixed in paraformaldehyde before being incubated in a blocking/permeabilization solution containing 2% (vol/vol) goat serum and 0.1% TritonX-100 for 30 min, followed by immunostaining with a secondary antibody (1/100 or 10 μg/mL of GAM-AF488) for 1–2 h in the same solution at room temperature. Coverslips were then washed three times in PBS and mounted. Samples were imaged using an Olympus FV-1000 confocal microscope with a 60× oil immersion objective. Software-recommended filters were used for each dye to acquire z-stacks with a 0.5-μm separation. Stacks were then merged using ImageJ.

Coimmunoprecipitation. Coimmunoprecipitation experiments were performed using primary cortical neurons. Neurons were separated into three groups: baseline, during NMDA application ("NMDA"), and 20 min after NMDA washout ("washout"). All three groups were initially incubated in blocking HBSS solution containing 100 μM 7CK (or 100 μM APV) for at least 7 min. Baseline neurons were maintained in HBSS solution; 25–40 μM NMDA was then added to the two other groups for ∼6 min. The NMDA group was lysed at the end of the NMDA application period; the washout group was lysed 20 min after washout of NMDA. Neurons were lysed in ice-cold lysis buffer [in mM: 50 Tris·HCl at pH 7.6, 150 NaCl, 2 EDTA, 1 PMSF; 1% Triton X-100, protease+phosphatase inhibitors (Sigma)]. Cell lysates were very briefly vortexed and centrifuged at 2,000 × *g* for 10 min. The supernatant was then collected and precleared using protein-A agarose beads (∼20 μL beads per sample; Pierce #22810) for ∼1.5–2 h at 4 °C. Lysates were spun down at ∼2,000 × *g* for 5 min to pellet the beads, which were then discarded. An aliquot from each supernatant was saved as the cell lysate. Protein concentrations were measured using the bicinchoninic acid (BCA) assay (Pierce) and normalized; generally, protein concentrations across all samples varied by less than 10%.

Lysates were mixed with ∼2–3 μL anti-GluN1 (MAB363, Millipore) or anti-GluN2B (#4212, Cell Signaling Technology) antibody per sample and gently inverted overnight at 4 °C. Immunoprecipitation was performed using protein-A agarose beads (20–30 μL) for 2–3 h at 4 °C with gentle inversion. Beads were pelleted at 2,000 × *g* for 5 min and washed 3 times using lysis buffer. NMDAR complexes were eluted in ∼30 μL Laemmli buffer and boiled for 5 min. Eluted samples were separated on either 7.5% or 4–20% Tris-Glycine gels (Bio-Rad, #456–1023 or #456–1096) and transferred onto polyvinylidene difluoride membranes (Millipore). Samples were blotted either overnight at 4 °C or at room temperature for 2 h with gentle rocking against GluN1, GluN2B, total CaMKII (#sc-5603; Santa Cruz Biotechnology), or phospho-CaMKII-Thr286 (#sc-12886-R; Santa Cruz Biotechnology). Immunoblotting was carried out in 5–7% milk or BSA in TBS-T. GluN1 and GluN2B antibodies were used at a 1:1,000–2,000 dilution. Total CaMKII levels were blotted at a 1:500–1,000 dilution, and phospho-CaMKII-Thr286 levels were blotted at a 1:200–400 dilution. Appropriate secondary antibodies (#sc-2004 and sc-2005; Santa Cruz Biotechnology) were used at a 1:5,000–10,000 dilution and blotted for 1 h at room temperature with gentle rocking. ECL Prime (GE Healthcare Lifesciences) was used for chemiluminescence. Immunoblots were visualized by film and analyzed using ImageJ.

ACKNOWLEDGMENTS. We thank Paul de Koninck and Luo Jian-hong for constructs. We would also like to thank Dr. J. Isaacson, Dr. A. Newton, Dr. M. Kunkel, Dr. N. Spitzer, Dr. D. Berg, and members of the R.M. laboratory for constructive comments. J.A. is supported by a scholarship from the Agency for Science, Technology and Research (A-STAR), Singapore.

1. Malenka RC, Bear MF (2004) LTP and LTD: An embarrassment of riches. *Neuron* 44(1): 5–21.
2. Malenka RC (1994) Synaptic plasticity in the hippocampus: LTP and LTD. *Cell* 78(4): 535–538.
3. Lisman J (1989) A mechanism for the Hebb and the anti-Hebb processes underlying learning and memory. *Proc Natl Acad Sci USA* 86(23):9574–9578.
4. Nabavi S, et al. (2013) Metabotropic NMDA receptor function is required for NMDA receptor-dependent long-term depression. *Proc Natl Acad Sci USA* 110(10):4027–4032.
5. Nabavi S, Fox R, Alfonso S, Aow J, Malinow R (2014) GluA1 trafficking and metabotropic NMDA: Addressing results from other laboratories inconsistent with ours. *Philos Trans R Soc Lond B Biol Sci* 369(1633):20130145.
6. Mayford M, Wang J, Kandel ER, O'Dell TJ (1995) CaMKII regulates the frequency-response function of hippocampal synapses for the production of both LTD and LTP. *Cell* 81(6):891–904.
7. Stein IS, Gray JA, Zito K (2015) Non-Ionotropic NMDA Receptor Signaling Drives Activity-Induced Dendritic Spine Shrinkage. *J Neurosci* 35(35):12303–12308.
8. Yang L, et al. (2004) A novel Ca^{2+}-independent signaling pathway to extracellular signal-regulated protein kinase by coactivation of NMDA receptors and metabotropic glutamate receptor 5 in neurons. *J Neurosci* 24(48):10846–10857.
9. Vissel B, Krupp JJ, Heinemann SF, Westbrook GL (2001) A use-dependent tyrosine dephosphorylation of NMDA receptors is independent of ion flux. *Nat Neurosci* 4(6): 587–596.
10. Tamburri A, Dudilot A, Licea S, Bourgeois C, Boehm J (2013) NMDA-receptor activation but not ion flux is required for amyloid-beta induced synaptic depression. *PLoS One* 8(6):e65350.
11. Nong Y, et al. (2003) Glycine binding primes NMDA receptor internalization. *Nature* 422(6929):302–307.
12. Kessels HW, Nabavi S, Malinow R (2013) Metabotropic NMDA receptor function is required for β-amyloid-induced synaptic depression. *Proc Natl Acad Sci USA* 110(10): 4033–4038.
13. Barria A, Malinow R (2002) Subunit-specific NMDA receptor trafficking to synapses. *Neuron* 35(2):345–353.
14. Cummings JA, Mulkey RM, Nicoll RA, Malenka RC (1996) Ca^{2+} signaling requirements for long-term depression in the hippocampus. *Neuron* 16(4):825–833.
15. Babiec WE, et al. (2014) Ionotropic NMDA receptor signaling is required for the induction of long-term depression in the mouse hippocampal CA1 region. *J Neurosci* 34(15):5285–5290.
16. Dore K, Aow J, Malinow R (2015) Agonist binding to the NMDA receptor drives movement of its cytoplasmic domain without ion flow. *Proc Natl Acad Sci USA* 112: 14705–14710.
17. Westphal RS, et al. (1999) Regulation of NMDA receptors by an associated phosphatase-kinase signaling complex. *Science* 285(5424):93–96.
18. Mulkey RM, Herron CE, Malenka RC (1993) An essential role for protein phosphatases in hippocampal long-term depression. *Science* 261(5124):1051–1055.
19. Strack S, Barban MA, Wadzinski BE, Colbran RJ (1997) Differential inactivation of postsynaptic density-associated and soluble Ca^{2+}/calmodulin-dependent protein kinase II by protein phosphatases 1 and 2A. *J Neurochem* 68(5):2119–2128.
20. Bayer KU, De Koninck P, Leonard AS, Hell JW, Schulman H (2001) Interaction with the NMDA receptor locks CaMKII in an active conformation. *Nature* 411(6839): 801–805.
21. Otmakhov N, et al. (2004) Persistent accumulation of calcium/calmodulin-dependent protein kinase II in dendritic spines after induction of NMDA receptor-dependent chemical long-term potentiation. *J Neurosci* 24(42):9324–9331.
22. Barria A, Malinow R (2005) NMDA receptor subunit composition controls synaptic plasticity by regulating binding to CaMKII. *Neuron* 48(2):289–301.
23. Dosemeci A, Reese TS (1993) Inhibition of endogenous phosphatase in a postsynaptic density fraction allows extensive phosphorylation of the major postsynaptic density protein. *J Neurochem* 61(2):550–555.
24. Barria A, Muller D, Derkach V, Griffith LC, Soderling TR (1997) Regulatory phosphorylation of AMPA-type glutamate receptors by CaM-KII during long-term potentiation. *Science* 276(5321):2042–2045.
25. Giese KP, Fedorov NB, Filipkowski RK, Silva AJ (1998) Autophosphorylation at Thr286 of the alpha calcium-calmodulin kinase II in LTP and learning. *Science* 279(5352): 870–873.

26. Hell JW (2014) CaMKII: Claiming center stage in postsynaptic function and organization. *Neuron* 81(2):249–265.
27. Fong YL, Taylor WL, Means AR, Soderling TR (1989) Studies of the regulatory mechanism of Ca^{2+}/calmodulin-dependent protein kinase II. Mutation of threonine 286 to alanine and aspartate. *J Biol Chem* 264(28):16759–16763.
28. Huang CC, Hsu KS (2001) Progress in understanding the factors regulating reversibility of long-term potentiation. *Rev Neurosci* 12(1):51–68.
29. Mayer ML, Westbrook GL, Guthrie PB (1984) Voltage-dependent block by Mg^{2+} of NMDA responses in spinal cord neurones. *Nature* 309(5965):261–263.
30. Sanderson TM, Collingridge GL, Fitzjohn SM (2011) Differential trafficking of AMPA receptors following activation of NMDA receptors and mGluRs. *Mol Brain* 4:30.
31. Kim MJ, et al. (2007) Synaptic accumulation of PSD-95 and synaptic function regulated by phosphorylation of serine-295 of PSD-95. *Neuron* 56(3):488–502.
32. Mullasseril P, Dosemeci A, Lisman JE, Griffith LC (2007) A structural mechanism for maintaining the 'on-state' of the CaMKII memory switch in the post-synaptic density. *J Neurochem* 103(1):357–364.
33. Lisman J, Raghavachari S (2015) Biochemical principles underlying the stable maintenance of LTP by the CaMKII/NMDAR complex. *Brain Res* 1621:51–61.
34. Kolodziej SJ, Hudmon A, Waxham MN, Stoops JK (2000) Three-dimensional reconstructions of calcium/calmodulin-dependent (CaM) kinase II alpha and truncated CaM kinase II alpha reveal a unique organization for its structural core and functional domains. *J Biol Chem* 275(19):14354–14359.
35. Stratton MM, Chao LH, Schulman H, Kuriyan J (2013) Structural studies on the regulation of Ca^{2+}/calmodulin dependent protein kinase II. *Curr Opin Struct Biol* 23(2):292–301.
36. Coultrap SJ, et al. (2014) Autonomous CaMKII mediates both LTP and LTD using a mechanism for differential substrate site selection. *Cell Reports* 6(3):431–437.